

See discussions, stats, and author profiles for this publication at: <https://www.researchgate.net/publication/249968269>

Charge Separation at the Molecular Monolayer Surface: Observation and Control of the Dynamics

ARTICLE *in* JOURNAL OF PHYSICAL CHEMISTRY LETTERS · MARCH 2012

Impact Factor: 7.46 · DOI: 10.1021/jz3002579

CITATIONS

7

READS

29

5 AUTHORS, INCLUDING:



Masahiro Shibuta

Keio University

20 PUBLICATIONS 100 CITATIONS

SEE PROFILE



Toyooki Eguchi

Keio University

85 PUBLICATIONS 858 CITATIONS

SEE PROFILE

Charge Separation at the Molecular Monolayer Surface: Observation and Control of the Dynamics

Masahiro Shibuta,^{†,‡} Naoyuki Hirata,[‡] Ryo Matsui,[‡] Toyoaki Eguchi,^{†,‡} and Atsushi Nakajima^{*,†,‡}

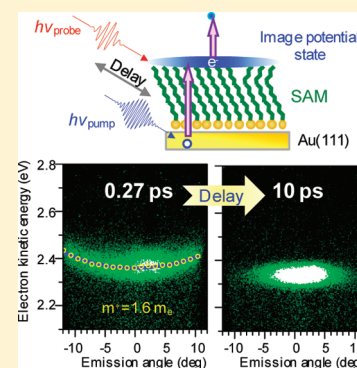
[†]Nakajima Designer Nanocluster Assembly Project, JST, ERATO, 3-2-1 Sakado, Takatsu-ku, Kawasaki 213-0012, Japan

[‡]Department of Chemistry, Faculty of Science and Technology, Keio University, 3-14-1 Hiyoshi, Kohoku-ku, Yokohama 223-8522, Japan

S Supporting Information

ABSTRACT: Charge separation dynamics relevant to an electron transfer have been revealed by time- and angle-resolved two-photon photoemission spectroscopy for an *n*-alkanethiolate self-assembled monolayer (SAM) on a Au(111) surface fabricated by a chemical-wet process. The electron was photoexcited into an image potential state located at 3.7 eV above the Fermi level (E_F), and it survived well for more than 100 ps on dodecanethiolate (C12)-SAM. The degree of electron separation is precisely controlled by selecting the length of the alkyl chain (C10–C18). We have also evaluated molecular conductivity at the specific electron energy of $E_F + 3.7$ eV. The tunneling decay parameter, β , was fitted by $\beta_{90\text{K}} = 0.097 \text{ \AA}^{-1}$ and $\beta_{\text{RT}} = 0.13 \text{ \AA}^{-1}$. These values were one order smaller than that at around E_F by conventional contact probe methods.

SECTION: Surfaces, Interfaces, Porous Materials, and Catalysis



The electron dynamics of charge separation from a metal substrate to the surface and interface is an important issue to create organic thin-film devices, such as gas sensors, solar cells, and transistors.^{1–4} The surface reactivity or functionality is triggered by injection of the excited electron into an unoccupied electronic state at the active site. Their quantum efficiencies are dominated by a degree of charge separation; nevertheless, the excited electron on the surface immediately relaxes to the metal substrate within the order of femtoseconds ($\text{fs} = 10^{-15} \text{ s}$).⁵ To overcome this challenge, an *n*-alkanethiolate self-assembled monolayer (C_{*n*}-SAM, where *n* is a number of carbon atoms) has attracted attention; the layer made of an alkyl chain is used as a thin insulator or inactivator.^{1–4} It is well recognized that the linkage arrangement with a strong Au–S bond forms a close-packed “standing-up” structure (Figure 1a) in which all alkyl chains are directed toward the vacuum.^{1,6,7} Owing to its high molecular packing and ordering, the alkyl layer of the SAM is considered as an efficient insulating molecular layer even at room temperature (RT). Such an insulating effect relevant to the charge separation dynamics in the SAM, however, has not been clarified in real time. In this study, we have tracked the highly separated photoexcited electron whose lifetime is close to 100 ps ($\text{ps} = 10^{-12} \text{ s}$) for the SAM on Au(111) prepared by a chemical-wet process, demonstrating that the degree of electron separation can be precisely controlled by the length of the alkyl chain. We also discuss the tunneling decay process relevant to the electron conductance for the insulating molecular layer at the specific

electron energy without any destructive effect, instead of contact probe methods.^{8,9}

In order to probe the charge separation dynamics, here, we employed two-photon photoemission (2PPE) spectroscopy in which an electron is pumped by a first photon ($h\nu_{\text{pump}}$) from an occupied state to an unoccupied state and is then photoemitted from the unoccupied state by a second probe photon, ($h\nu_{\text{probe}}$) (Figure 1a).^{5,10} By scanning the delay between the pump and probe pulses, the time evolution of the excited electron is detected with femtosecond time resolution (time-resolved (TR)-2PPE). Figure 1b shows the TR-2PPE spectra for a C12-SAM (see the Supporting Information for molecular ordering of the sample) with various time delays. At zero delay, a small unoccupied state was observed at 3.7 eV above the Fermi level (E_F), coincident with the 2PPE signals from a hot electron below the accessible intermediate energy of $E_F + h\nu_{\text{pump}}$. With a nonzero time delay, the unoccupied state grew significantly and achieved a maximum intensity at about 4 ps. Moreover, the unoccupied state was observed even at 200 ps after the pump pulse. These results indicate that the photoexcited electron is trapped in the unoccupied state and is effectively isolated from the metal substrate.

The character of the unoccupied state that we obtained in Figure 1b can be examined by its polarization dependence (Figure 2); a p-polarized probe pulse is definitely required to

Received: March 3, 2012

Accepted: March 22, 2012

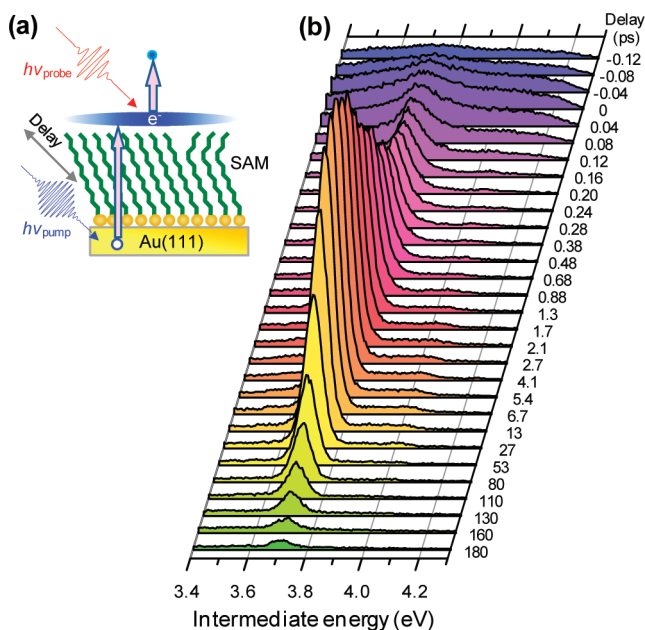


Figure 1. (a) Schematic description of the close-packed standing-up structure of C_n -SAM and the 2PPE process. (b) TR-2PPE spectra (surface normal emission) for a C12-SAM on Au(111) at 90 K. Photon energies were $h\nu_{\text{pump}} = 4.23$ eV and $h\nu_{\text{probe}} = 1.41$ eV. The horizontal axis is the intermediate energy relative to E_F . Time delays between both photons are noted on the right-hand side.

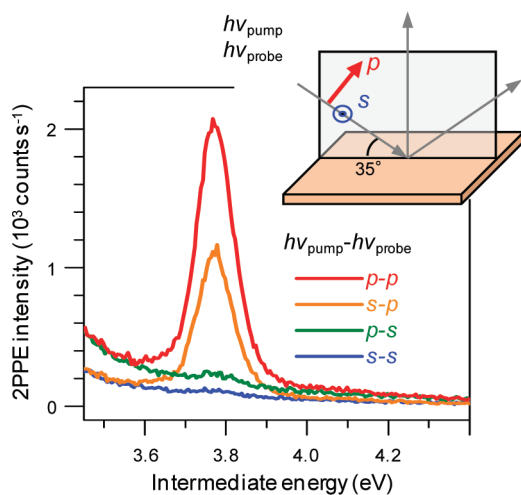


Figure 2. Polarization dependence of the 2PPE spectra at a 4 ps delay. The inset illustrates the light polarization configurations of both $h\nu_{\text{pump}}$ and $h\nu_{\text{probe}}$.

excite a photoelectron (red and orange lines). The polarization selectivity for the probe pulse indicates that the photoexcited electron in the unoccupied state is bound to the surface normal direction but not to the surface parallel.^{5,10} Considering the work function of the SAM (4.25 ± 0.02 eV), the unoccupied state is located at about 0.55 eV below the vacuum level. From the above results, we have attributed the unoccupied state to the first image potential state (IPS)^{11–13} formed on the SAM.

Lindstrom et al. observed the IPS formed on the C6-SAM but only for the “lying-down” phase and not for the standing-up phase in ref 14. In the same paper, they also reported about the σ^* state derived from Au–S chemical bonds for both phases. In our case, the σ^* state can be observed with single-color 2PPE

($h\nu_{\text{pump}} = h\nu_{\text{probe}} = 4.23$ eV) at a slightly lower binding energy than that of the IPS (see the Supporting Information). Although the σ^* state and the IPS have not been observed simultaneously, they can be distinguished clearly from their spectral and temporal features. The σ^* state is observed independently of the light polarization and has a very short lifetime (< 20 fs) and very small energy dispersion.¹⁴ The IPS observed in the present study, on the other hand, shows distinct polarization dependence, as indicated in Figure 2, and has a long lifetime (~ 100 ps) and clear energy dispersion, which are discussed in detail below.

It is known that the IPS has a two-dimensional free-electron-like nature.^{11–13} Figure 3a and b shows the angle-resolved

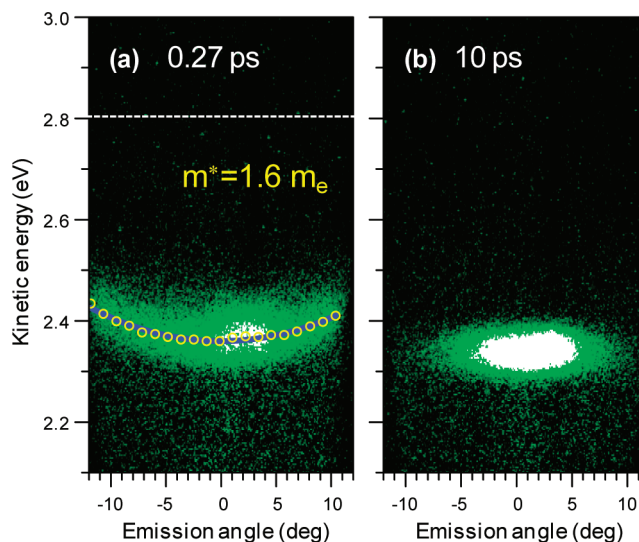


Figure 3. AR-2PPE image ($h\nu_{\text{pump}} = 4.23$ eV, $h\nu_{\text{probe}} = 2.82$ eV) of a C12-SAM taken at delay times of 0.27 (a) and 10 ps (b). A free-electron-like dispersion is observed in (a) with an effective mass of $1.6 m_e$. The electrons excited below $E_F + h\nu_{\text{pump}}$ (dotted line in (a)) subsequently relax toward the band minimum ($k_{\parallel} = 0$), as shown in (b).

(AR)-2PPE spectra measured at delays of 0.27 and 10 ps, respectively. The horizontal and vertical axes are the emission angle (θ) with respect to the surface normal and kinetic energy (E_k) of the photoelectron, respectively. At 0.27 ps, a free-electron-like dispersion was observed. The surface parallel momentum of the photoelectron (k_{\parallel}) is connected to the energy by $k_{\parallel} = (2m_e E_k)^{1/2} \sin \theta / \hbar$, where m_e is the mass of a free electron of $1 m_e$. By fitting a parabolic function of $E_k = E_0 + \hbar^2 k_{\parallel}^2 / (2m^*)$, the effective mass (m^*) of the excited electron is evaluated to be $1.6 m_e$. This value is slightly heavier than the free electron. The effective mass of the IPS is affected by hybridization with localized states such as molecular unoccupied states or electron affinity⁵ and surface lateral inhomogeneity.¹⁵ In the SAM case, the former is not so predominant because of the wide band gap in the alkyl chain layer. The intrinsic defect's so-called “etch pit”⁷ (see also the Supporting Information) may affect the heavier m^* .

At a time delay of 10 ps (Figure 3b), the 2PPE signal is strongly enhanced near normal emission ($k_{\parallel} = 0$). This result shows that the electrons are initially populated at the image potential band with all of the parallel momenta (Figure 3a) and are subsequently relaxed toward the band minimum ($k_{\parallel} = 0$) through an intraband transition. This intraband relaxation

induces the initial increase of the 2PPE signal intensity observed in the few picosecond region in Figure 1b because the spectra shown in Figure 1b are obtained by detecting emitted electrons at $k_{\parallel} = 0$ with a small acceptance angle ($\pm 4^\circ$). Harris and co-workers reported similar behavior for the IPS-mediated self-trapped state in *n*-heptane/Ag(111).¹⁶ They observed the maximal intensity at a delay time of ~ 1 ps and extracted the rise time (360 ± 140 fs) and decay time (1600 ± 200 fs). In the case of the present system, it shows a similar rise time but a much longer decay time at $k_{\parallel} = 0$ due to the long lifetime of IPS, as discussed later in Figure 4. Such a long

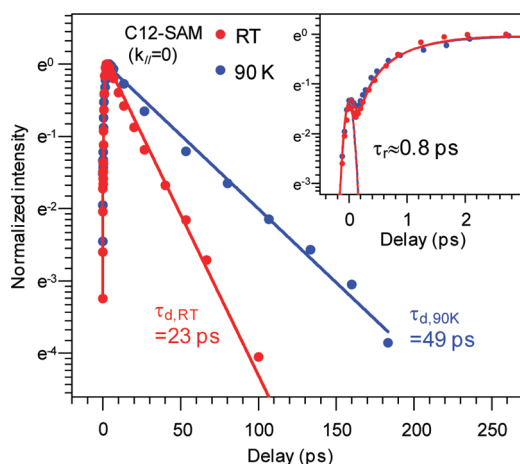


Figure 4. Intensity traces of the IPS of a C12-SAM at RT (red circles) and 90 K (blue circles), providing the rise and decay times. The inset shows a magnified trace for delay times < 3 ps. The dashed line represents the coherent 2PPE component, which is in agreement with a cross-correlation of pump and probe pulses. The 2PPE trace is fitted by the sum of the coherent 2PPE component and the electron population in the unoccupied state $P(t)$, which is described by $P(t) \propto [\exp(-t/\tau_r) - \exp(-t/\tau_d)]$ from the simple rate equation.

lifetime of the IPS causes the delayed maximum at 4 ps and the significant enhancement of photoemission intensity at $k_{\parallel} = 0$.

As can be seen in Figure 3b, the 2PPE intensity strongly depends on the emission angle; the effective signal comes from only around $k_{\parallel} = 0$. The IPS electron is therefore still delocalized at even 10 ps after excitation. Our result implies that electrons in the IPS are not trapped in any localized state like self-trapping¹⁶ or electron solvation states.¹⁷ If such localized states are formed, it should have small energy dispersion and small emission angle dependence of the 2PPE intensity. A slight energetic stabilization (~ 20 meV) at $k_{\parallel} = 0$ at a time delay may be due to a modification of the surface potential or the geometric configuration by the excited electrons.

One may be curious why such a great many electrons can be excited to the IPS. Because the electron transition probability from the metal substrate to the IPS depends on a degree of wave function penetration into the substrate, the intensity of IPS formed on the thick alkyl layer of the SAM should be small. A possible explanation for the large IPS intensity is electron population through intermediate states formed in the alkyl layer. Muntwiler et al. have reported that the interfacial resonance (IR) is formed in the film for the standing-up phase of alkanethiolate SAMs at a binding energy of 4.2 eV above E_F .¹⁵ While the IR is not observed in this study maybe due to lower photon energy compared to that in previous work

($h\nu_{\text{pump}} = 4.65$ eV, $h\nu_{\text{probe}} = 1.55$ eV), we may say that the electrons excited from the substrate initially occupy the IR and then immediately transfer to the IPS by interband transition. Because the IR is spatially located at the metal–SAM interface, it is possible to populate more electrons to the IR than the IPS. It seems that almost all of the electron excitation to IPS through IR occurs in a relatively short time just after the pumping because the integrated intensities of the 2PPE spectra shown in Figure 3a and b are much the same (Figure 3b/a = 1.08). It is consistent with a short lifetime (< 20 fs) of IR.¹⁸ Slight increase of the integrated intensity in Figure 3b can be attributed to the limited detection angle of Figure 3 ($\pm 12^\circ$) compared to the widely dispersed IPS up to about $\pm 20.5^\circ$, which was determined by the accessible intermediate energy (a white broken line in Figure 3a).

Momentum-resolved electron dynamics at a picosecond time scale has been reported for semiconductors^{19,20} but not for a molecular monolayer system. For a quantitative analysis of the photoexcited electron dynamics, the 2PPE intensities of the IPS near $k_{\parallel} = 0$ were plotted against the delay times for the sample temperatures of RT (red circles) and 90 K (blue circles), as shown in Figure 4. By assuming the simple rate equation, the rise time τ_r and decay time τ_d were fitted by 0.84 and 49 ps for the sample temperatures of 90 K, respectively. The rise time at $k_{\parallel} = 0$, which is independent of the temperature, represents the period for the intraband relaxation on adsorbed surfaces.^{21,22} In contrast to the rise time, the decay time of the IPS is substantially longer than the known values of 10.3 ps for 5 monolayer (ML) of Ar on Cu(100) at 18 K²³ or 17.6 ps for a 3 ML *n*-heptane layer on Ag(111) at 110 K.¹³ The electron dynamics in such IPS states have been studied with a dielectric continuum model; the IPS electron efficiently survives when the IPS is located in the projected band gap of the substrate and the adsorbate has a small or negative electron affinity.^{11–13,23} Hence, this model is also applicable to the present SAM case. Compared to previous studies, however, the striking difference found here is the longer lifetime of 20 ps at RT; nevertheless, the thickness of the alkyl layer of a C12-SAM (12.1 Å) is similar to that of the 5 ML Ar (13.5 Å)²³ and 3 ML *n*-heptane (12 Å).¹³

The longer lifetime can be ascribed to the fact that the SAM film preserves a uniform, rigid, and dense alkyl comb even at RT because the SAM is formed not only through chemical bonding between gold and sulfur atoms but also by nonbonding interactions between alkyl chains, resulting in the formation of a well-packed and molecularly ordered layer. At low temperature (< 160 K), much longer living excited electrons up to minutes have been observed on ice/metal and ammonia/metal surfaces.²⁴ Solvated electrons in such polar molecules trap and stabilize excited electrons. In the case of the SAM film, solvated electrons by slightly polarized C–H bonds might partially contribute to the long lifetime of the IPS electrons²⁵ but should not be dominant because the observed IPS electrons are delocalized after a sufficiently long time (delay time > 10 ps). If the IPS electron is trapped by a specific H atom, it should give a localized feature without showing energy dispersion in AR-2PPE. More experimental and theoretical approaches are needed for further understanding.

The use of a SAM enabled us to investigate the electron dynamics on an insulating layer over a wide range of temperatures. The lifetime decreased to 23 ps at RT, suggesting that thermodynamic disordering of the SAM or vibronic coupling affects the decay dynamics (Figure 4). Briefly, with increasing temperature, the structure of the C n -SAM fluctuates,

and the “frozen” alkyl comb starts to waver, which is well-known to produce “gauche defects”.^{1,26}

Because the thickness of the ordered layer can be modified systematically by varying the chain length, it is possible to control the degree of electron separation by the thickness of the insulating layer. Figure 5 shows the decay times at RT and 90 K

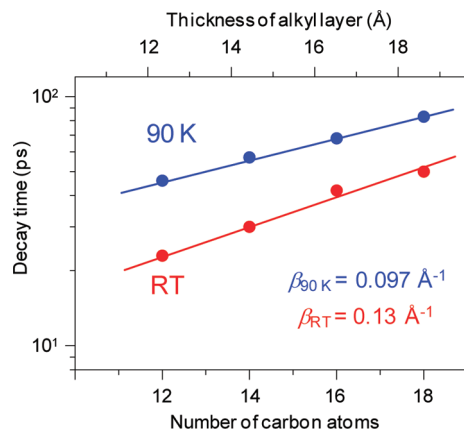


Figure 5. Chain length dependence of the decay times at RT (red circles) and 90 K (blue circles) to evaluate the tunneling decay parameter, β . The lower and upper horizontal axes represent the number of carbon atoms and the thickness of the alkyl layer in Å, estimated from the alkyl chain length minus the Au–S bond and a tilt angle of $\sim 30^\circ$.^{1,26}

as a function of the alkyl chain length. The decay time increased with chain length, although the energy position of the IPS is almost independent of chain length (not shown). This result clearly indicates that the lifetime of the photoinduced electron can be precisely controlled by changing the alkyl layer thickness. From the thickness dependence of the lifetime, the electron tunneling probability through the SAM can be estimated within the WKB approximation; the lifetime is described as a function of the alkyl layer thickness l by $\tau_d(l) \propto \exp(\beta \cdot l)$, where β is the tunneling decay parameter. Our results were well fitted with $\beta_{90\text{ K}} = 0.097 \text{ Å}^{-1}$ and $\beta_{\text{RT}} = 0.13 \text{ Å}^{-1}$, as shown in Figure 5. These values are one order smaller than previously reported values (about 1 Å^{-1}).^{8,9} This is because we have observed the electron tunneling process at the IPS, that is, 3.7 eV above E_F . In the past decades, molecular conductance has been extensively studied based on current–voltage (I – V) measurements by making a conductor–molecule–conductor junction.^{8,9} The β values have been conventionally evaluated with I – V curves in the vicinity of zero-bias voltage. Organic molecules, however, do not show ohmic character over a wider voltage range due to their intrinsic density of states and electron affinities. In addition, the strong electric field at higher bias voltages may modify the character of a molecule, both structurally and electronically. Therefore, it is difficult to evaluate the tunneling conductance for a specific electron energy, although it is important to know this for electron injection to trigger various surface functionalities. The analytical method described here based on the present TR-2PPE study can access such a high energy region without any destructive effect and will be widely applicable to the evaluation of the electronic properties of various surfaces.

In summary, we have demonstrated precise control of charge separation using the free-electron-like IPS formed on a C n -SAM. After the electrons excited with purely parallel momenta

relax to the band minimum, the electrons are well-separated in the molecularly ordered SAM and surprisingly survive for more than 100 ps without any energetic relaxation. Real-time observation of the electron dynamics by using TR- and AR-2PPE helps us to understand the importance of molecularly ordered surfaces and further the use of surface functionality to the expanding field of nanotechnology.

METHODS

All 2PPE experiments were performed in an ultrahigh vacuum (UHV) chamber where the base pressure was $<1 \times 10^{-8}$ Pa. The third harmonic (TH, $h\nu = 4.23 \text{ eV}$) of a titanium–sapphire laser generated by a couple of β -BaB₂O₄ crystals was used as a $h\nu_{\text{pump}}$, and its fundamental ($h\nu = 1.41 \text{ eV}$) or second harmonic ($h\nu = 2.82 \text{ eV}$) was employed as a $h\nu_{\text{probe}}$. The repetition rate of 76 MHz was enough to maintain the quality of the SAM sample and to avoid a space charge effect. The light was focused onto the sample in the UHV chamber with a $f = 400 \text{ mm}$ concave mirror; the diameter of the spot size on the sample was as large as 0.1 mm for a TH pulse. The incident laser powers, especially for the ultraviolet TH pulse, were very carefully controlled below 13 pJ/pulse to avoid damage to the SAM. Photoelectrons emitted from the sample via two-photon processes were detected by a hemispherical energy analyzer (VG: Alpha110, equipped with five channeltrons, or VGSCIENTA: R-3000, equipped with a two-dimensional microchannel plate detector). The total energy resolutions of the 2PPE setups were about 20 meV. The optical delay was controlled by a precision stage where the minimum step is 100 nm, which turned at 0.67 fs per step. The time resolution of our setup was less than 30 fs. The polarizations of pump and probe pulses were always p-polarized, except for the experiment of polarization dependence (Figure 2). The sample temperature for 2PPE experiments was controlled between 90 and 300 K.

The Au(111) single-crystal substrate was cleaned by repeated cycles of Ar⁺ ion sputtering (0.6 kV, $\sim 3 \mu\text{A}$, 15 min) and annealing (770 K, 30 min). The cleanliness of the surface was confirmed by a 2PPE measurement, which confirmed a work function of 5.5 eV and a sharp Shockley surface state located at $E_F - 0.4 \text{ eV}$. In the SAM preparation, a chemical process was used; the cleaned Au(111) substrate was immersed in an ethanolic 0.5 mM *n*-alkanethiol solution for 20 h. After that, the sample was rinsed with pure ethanol and immediately introduced to the UHV chamber for 2PPE measurements through a load lock chamber.

ASSOCIATED CONTENT

Supporting Information

STM images of the SAM and additional supporting text and figure. This material is available free of charge via the Internet at <http://pubs.acs.org>.

AUTHOR INFORMATION

Corresponding Author

*E-mail: nakajima@chem.keio.ac.jp. Phone: +81-45-566-1712. Fax: +81-45-566-1697.

Notes

The authors declare no competing financial interest.

ACKNOWLEDGMENTS

The authors sincerely thank Dr. Masato Nakaya and Mr. Masaya Shikishima for performing the scanning tunneling

microscopy to ensure the uniformity of the SAM samples. This work is partly supported by the Science Research Promotion Fund from the Promotion and Mutual Aid Corporation for Private Schools of Japan.

REFERENCES

- (1) Love, J. C.; Estroff, L. A.; Kriebel, J. K.; Nuzzo, R. G.; Whitesides, G. M. Self-Assembled Monolayer of Thiolates on Metals as a Form of Nanotechnology. *Chem. Rev.* **2005**, *105*, 1103–1170.
- (2) Schreiber, F. Self-Assembled Monolayers: from ‘Simple’ Model Systems to Biofunctionalized Interfaces. *J. Phys.: Condens. Matter* **2004**, *16*, R881–R900.
- (3) Yip, H.-L.; Hau, S. K.; Baek, N. S.; Ma, H.; Jen, A. K.-Y. Polymer Solar Cells That Use Self-Assembled-Monolayer Modified ZnO/Metals as Cathodes. *Adv. Matter.* **2008**, *20*, 2376–2382.
- (4) Halik, M.; Klauk, H.; Zschieschang, U.; Schmid, G.; Dehm, C.; Schütz, M.; Maisch, S.; Franz, E.; Brunnbauer, M.; Stellacci, F. Low-Voltage Organic Transistors with an Amorphous Molecular Gate Dielectric. *Nature* **2004**, *431*, 963–966.
- (5) Zhu, X. Y. Electronic Structure and Electron Dynamics at Molecule–Metal Interfaces: Implications for Molecule-Based Electronics. *Surf. Sci. Rep.* **2004**, *56*, 1–83.
- (6) Vericat, C.; Vela, M. E.; Benitez, G. A.; Martin Gago, J. A.; Torrelles, X.; Salvarezza, R. C. Surface Characterization of Sulfur and Alkanethiol Self-Assembled Monolayer on Au(111). *J. Phys.: Condens. Matter* **2006**, *18*, R867–R900.
- (7) Maksymovych, P.; Voznyy, O.; Dougherty, D. B.; Sorescu, D. C.; Yates, J. T. Jr. Gold Adatom as a Key Structural Component in Self-Assembled Monolayers of Organosulfur Molecules on Au(111). *Prog. Surf. Sci.* **2010**, *85*, 206–240.
- (8) Salomon, A.; Cahen, D.; Lindsay, S.; Tomfohr, J.; Engelkes, V. B.; Frisbie, C. D. Comparison of Electronic Transport Measurements of Organic Molecules. *Adv. Mater.* **2003**, *15*, 1881–1890.
- (9) Wold, D. J.; Frisbie, C. D. Fabrication and Characterization of Metal–Molecule–Metal Junctions by Conducting Probe Atomic Force Microscopy. *J. Am. Chem. Soc.* **2001**, *123*, 5549–5556.
- (10) Szymansky, P.; Garrett-Roe, S.; Harris, C. B. Time- and Angle-Resolved Two-Photon Photoemission Studies of Electron Localization and Solvation at Interfaces. *Prog. Surf. Sci.* **2005**, *78*, 1–39.
- (11) Harris, C. B.; Ge, N.-H.; Lingle, R. L. Jr.; McNeill, D. Femtosecond Dynamics of Electrons on Surfaces and at Interfaces. *Annu. Rev. Phys. Chem.* **1997**, *48*, 711–744.
- (12) Hotzel, A. Electron Dynamics of Image Potential States in Weakly Bound Adsorbate Layers: A Short Review. *Prog. Surf. Sci.* **2007**, *82*, 336–354.
- (13) Güttele, J.; Höfer, U. Femtosecond Time-Resolved Studies of Image-Potential States at Surfaces and Interfaces of Rare-Gas Adlayers. *Prog. Surf. Sci.* **2005**, *80*, 49–91.
- (14) Lindstrom, C. D.; Muntwiler, M.; Zhu, X.-Y. Electron Transport Across the Alkanethiol Self-Assembled Monolayer/Au(111) Interface: Role of the Chemical Anchor. *J. Phys. Chem. B* **2005**, *109*, 21492–21495.
- (15) Yang, A.; Shipman, S. T.; Garrett-Roe, S.; Johns, J.; Strader, M.; Szymanski, P.; Muller, E.; Harris, C. Two-Photon Photoemission of Ultrathin Films PTCDA Morphologies on Ag(111). *J. Phys. Chem. C* **2008**, *112*, 2506–2513.
- (16) Ge, N.-H.; Wong, C. M.; Lingle, R. L. Jr.; McNeill, J. D.; Gaffney, K. J.; Harris, C. B. Femtosecond Dynamics of Electron Localization at Interfaces. *Science* **1998**, *279*, 202–205.
- (17) Stähler, J.; Meyer, M.; Bovensiepen, U.; Wolf, M. Solvation Dynamics of Surface-Trapped Electrons at NH₂ and D₂O Crystallites Adsorbed on Metals: from Femtosecond to Minute Time Scales. *Chem. Sci.* **2011**, *2*, 907–916.
- (18) Muntwiler, M.; Lindstrom, C. D.; Zhu, X.-Y. Delocalized Electron Resonance at the Alkanethiolate Self-Assembled Monolayer/Au(111) Interface. *J. Chem. Phys.* **2006**, *124*, 081104–1–3.
- (19) Haight, R. Electron Dynamics at Surfaces. *Surf. Sci. Rep.* **1995**, *21*, 275–325.
- (20) Weinelt, M.; Kutschera, M.; Fauster, Th.; Rohlfing, M. Dynamics of Exciton Formation at the Si(100) c(4 × 2) Surface. *Phys. Rev. Lett.* **2004**, *92*, 126801–1–4.
- (21) Roe, S. G.; Shipmann, S. T.; Szymanski, P.; Strader, M. L.; Yang, A.; Harris, C. B. Ultrafast Electron Dynamics at Metal Interfaces: Intraband Relaxation of Image State Electron as Friction. *J. Phys. Chem. B* **2005**, *109*, 20370–20378.
- (22) Hotzel, A.; Wolf, M.; Gauyacq, J. P. Phonon-Mediated Intraband Relaxation of Image-State Electrons in Adsorbate Overlayers: N₂/Xe/Cu(111). *J. Phys. Chem. B* **2000**, *104*, 8438–8455.
- (23) Berthold, W.; Rebentrost, F.; Feulner, P.; Höfer, U. Influence of Ar, Kr, and Xe Layers on the Energies and Lifetimes of Image-Potential States on Cu(100). *Appl. Phys. A: Mater. Sci. Process.* **2004**, *78*, 131–140.
- (24) Bovensiepen, U.; Gahl, C.; Stähler, J.; Bockstedte, M.; Meyer, M.; Baletto, F.; Scandolo, S.; Zhu, X.-Y.; Wolf, M. A Dynamic Landscape from Femtoseconds to Minutes for Excess Electrons at Ice–Metal Interfaces. *J. Phys. Chem. C* **2009**, *113*, 979–988.
- (25) Zhao, J.; Li, B.; Onda, K.; Feng, M.; Petek, H. Solvated Electrons on Metal Oxide Surfaces. *Chem. Rev.* **2006**, *106*, 4402–4427.
- (26) Dubois, L. H.; Nuzzo, R. G. Synthesis, Structure, and Properties of Model Organic Surface. *Annu. Rev. Phys. Chem.* **1992**, *43*, 437–463.